Catalysis Today 145 (2009) 169–175

Contents lists available at ScienceDirect

Catalysis Today

journal homepage: www.elsevier.com/locate/cattod

Enhanced selective glycerol oxidation in multiphase structured reactors

Stephen D. Pollington [a,*], Dan I. Enache [b], Philip Landon [b], Sankar Meenakshisundaram [b], Nikolaos Dimitratos [b], Alison Wagland [c], Graham J. Hutchings [b,*], E. Hugh Stitt [a]

[a] Johnson Matthey Technology Centre, P.O. Box 1, Belasis Avenue, Billingham TS23 1LB, UK
[b] School of Chemistry, Cardiff University, Main Building, Park Place, Cardiff CF10 3AT, UK
[c] Johnson Matthey Technology Centre, Blount's Court, Sonning Common, Reading RG4 9NH, UK

ARTICLE INFO

Article history:
Available online 4 June 2008

Keywords:
Multiphase reactions
Glycerol oxidation
Gold catalyst
Slurry bubble column
Continuous flow structured reactors

ABSTRACT

Gold catalysis has potential for multiphase oxidation using molecular oxygen but hitherto has been evaluated only in batch autoclaves. The use of continuous flow structured reactors for the oxidation of glycerol under mild conditions using a gold/carbon catalyst is demonstrated. Both monolith and meso-scale structured downflow slurry bubble column designs lead to a significant enhancement in the reaction rate over autoclave studies which is an order of magnitude greater for the gold/carbon coated monolith, and two orders of magnitude for the meso-scale structured downflow slurry bubble column reactor. A change in the reaction products is observed between structured monolith reactor and meso-structured slurry bubble column reactor. The monolith and autoclave data show very high selectivity to glyceric acid, whereas the thin channel slurry bubble column yields approximately equal quantities of dihydroxyacetone and glyceric acid under similar conditions. Since the same batch of catalyst is used for both the autoclave and the meso-scale structured downflow slurry bubble column reactor, the difference in selectivity cannot be attributed to a particle size effect. The difference in selectivity is attributed to enhanced interaction between bubbles and particles from structuring gas–liquid–solid reacting flows in thin channels or capillaries.

1. Introduction

The use of coated catalyst monolithic systems has been widely proposed for fine chemicals reactions [1–4]. Fixed bed type systems, despite their many advantages, do not, however, offer the same flexibility for multi-product operation as the fine chemicals industry currently enjoys with the stirred tank and slurry catalysts. Intensified reactors such as the Oscillatory Flow Baffled Reactor [5] and the BHR Group FLEX reactor [6] have been employed in the fine chemicals manufacturing industry. However, these reactors again utilize slurry catalysts rather than trickle bed or monolith reactor and thus, retain the unit flexibility that the fine chemical industry craves. Process intensification routes such as the use of a flowing three phase reacting system in thin channels have been investigated for heterogeneously catalyzed hydrogenation as a means to capitalize on the benefits of structured reactors while retaining the advantages of slurry catalysts [7,8]. These studies focused on single capillary channel systems being representative of commercial processes, which would comprise of many channels using the scale-out approach used in micro-channel and monolith applications [9]. The question of heat transfer availability for scale-out for mm channels has been addressed by considering shell and tube type arrangement and compact heat exchanges. A recent study has extended the single capillary work [7] and looked at the use of heat exchange (HEx) reactors where different flow channel designs of HEx reactors were used for evaluating the feasibility of scaling out the process [10]. This multichannel system would have excellent heat transfer and temperature control, enhanced gas–liquid–solid interaction, increased rate and kinetic control, reduced equipment inventory and the flexibility of a multi-product batch plant.

However, the question remains; is the use of flowing three phase (slurry–liquid–gas) system in thin channels more productive than immobilizing the catalyst onto the walls of the thin channel as in a coated monolith? The hydrodynamics of gas–liquid–solid systems are complex and the literature contains a number of studies that infer significant differences between a gas–liquid monolith and a slurry bubble column reactor (SBCR) structured at the bubble scale. For example, Kreutzer et al. [11] have investigated the characteristics of pressure drop in capillaries for liquid–gas systems and identified conditions where

* Corresponding authors.
E-mail addresses: steve.pollington@matthey.com (S.D. Pollington), hutch@cf.ac.uk (G.J. Hutchings).

0920-5861/$ – see front matter © 2008 Elsevier B.V. All rights reserved.
doi:10.1016/j.cattod.2008.04.020

all channels in a monolith behave essentially identically in downflow mode. Some channels will have slugs or bubbles of different lengths but the speed of these slugs or bubbles traveling downward will be similar. The limiting mass-transfer step for the gas is through the film between the bubble or slug and the channel wall. This will be of comparable thickness for slugs and bubbles regardless of slug/bubble length. However, this model does not take into account the influence of solid particles in these systems traveling co-currently. Krishna observed significant effects in "trailing bubbles" with fluid flow-field perturbations in the interstitial region that will dominate capillary flow [12]. Particles have been observed to exert a substantial influence on bubble behavior [12,13]. Furthermore, particle–bubble interaction has been observed to lead to enhanced transport and reaction rates [14]. There is clearly a significant interaction between bubbles and particles, and meso-scale structuration may therefore lead to enhancement of the benefits observed in multiphase catalyzed monoliths.

Most studies with monolith systems operate at higher liquid–gas velocities to induce slug-flow or Taylor flow regime. This flow regime is reported to give high mass-transfer characteristics, but to achieve this superficial liquid velocities in excess of 0.1 m s^{-1} are reputed to be required [1]. When using low liquid and gas superficial velocities it is difficult to establish the flow regime, and there does not seem to be general agreement in the literature. Flow maps have been constructed for co-current gas–liquid flow in capillary channels that indicate that a number of flow regions, including slug flow (Taylor flow), are observed at low liquid velocities and high gas velocities. Kapteijn et al. [1] have stated that operation at liquid superficial velocities of $<$0.1 m s^{-1} moves the hydrodynamic regime out of slug flow into bubbly flow. The probable reason for the discrepancies in the literature is the fact that it is difficult to measure Taylor flow in a monolithic structure because of the small channel size and system opacity. The only experimental technique with adequacy of both temporal and spatial resolution to quantitatively measure gas–liquid flow in multi-channel systems is magnetic resonance imaging (MRI). Studies using this approach [15,16] indicate that Taylor flow is obtained at liquid velocities less than 10 mm s^{-1}. Similar observations of Taylor flow at low superficial velocities have been made by Tsoligkas et al. [17] for a reacting system.

In this article we report experimental data for the oxidation of glycerol using carbon supported gold catalysts in slurry and monolith form. Glycerol is a highly functionalized molecule that is readily available from biosubstainable sources. For example, it is produced as a by-product from biodiesel manufacture. A large number of products can be obtained from oxidation of glycerol (Fig. 1), however, control of the reaction selectivity is a requirement of the fine chemicals industry. This is particularly true of the chemical transformation of glycerol into useful products. As the production of biodiesel increases, due to legislation requiring that significant proportions of transportation fuel is derived from bio-sustainable resources, massive quantities of glycerol will be available for industrial use. Heterogeneous catalytic systems have been advocated as an alternative to the traditional oxidation processes used in the fine chemical industry, which suffer from several drawbacks, including poor selectivity and the use of environmentally unfriendly reagents based on dichromate and permanganate [18–22]. Studies on oxidation of glycerol with oxygen in aqueous solution have been conducted on supported catalysts based on palladium, platinum and gold [23–37]. Gold was once considered to be relatively catalytic inactive compared with precious metal systems but has recently attracted much interest for hydrogenation and oxidation reactions in both heterogeneous and homogenous form [23]. Typical oxidation products over palladium and platinum catalysts are either glyceric acid or dihydroxyacetone but subsequent oxidation takes place [24–27]. The nature of the mass-transfer regime is likely to affect both rate and selectivity, and the reaction mechanism may dictate the need for a particular mass-transfer regime. The mechanism of glycerol oxidation over platinum and palladium catalysts has been shown to involve oxidative dehydrogenation [24]. If the rate of oxygen mass transfer is too high over-oxidation of the metal can occur leading to catalyst deactivation. Further oxidation of glyceric acid or dihydroxyacetone to yield products such as tartronic acrid and oxalic acid also occurs [27]. Recently gold on carbon has been advocated as a very active and selective catalyst for the oxidation of glycerol [28–37], since our initial discovery that gold supported on carbon was very selective for the oxidation of glycerol to glycerate. In contrast to oxidation using palladium and platinum catalysts, glycerol oxidation over gold requires the presence of base, and this is considered essential in assisting with the rate-limiting deprotonation step [29]. Gold gives the possibility of higher reaction rates due to its increased tolerance to oxygen availability and resistance to over-oxidation. Previous batch stirred reactor studies with pure oxygen using carbon supported gold slurry catalysts have shown that high conversion of glycerol can be obtained with high selectivity to glyceric acid [28,29]. This study extends that work on the oxidation of glycerol with gold catalyst under mild conditions by employing air in flowing, structured reactors where an enhanced mass-transfer effect can be created.

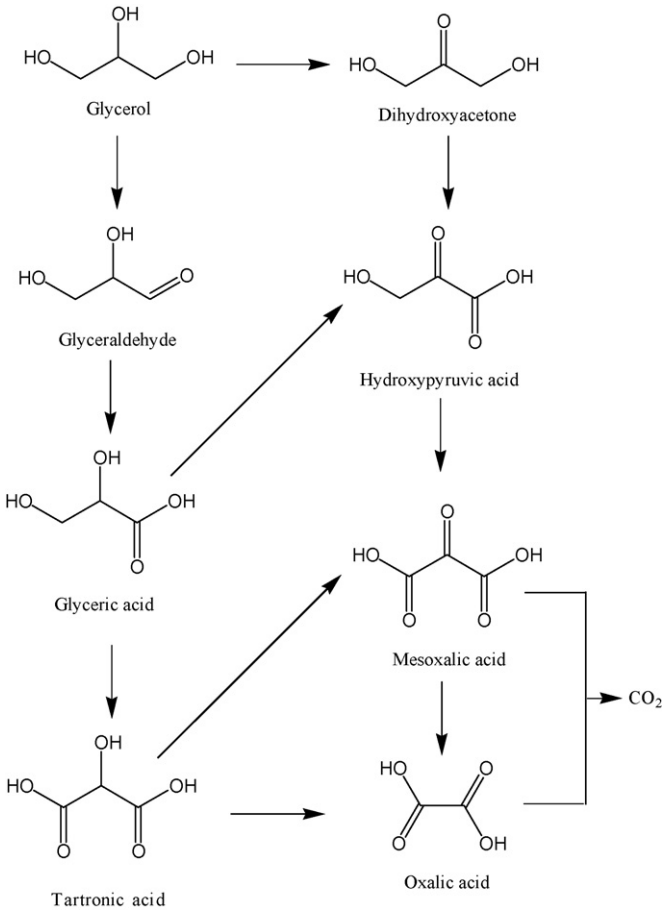

Fig. 1. Reaction schematic of possible products from glycerol oxidation.

2. Experimental

2.1. Catalyst synthesis

The 1 wt%Au/C catalyst was made as previously described [28] by adding chloroauric acid (Johnson Matthey) to an aqueous suspension of graphite (Johnson Matthey) and reducing with formaldehyde. A gold on carbon monolith catalyst was made using cordierite monoliths (62 channels per cm^2 (or 400 cpsi)). The monoliths were prepared by soaking a cordierite monolith in a slurry of graphite, phenol formaldehyde resin and a suitable solvent to reduce the viscosity. After blowing the excess slurry from the monolith with compressed air, it was dried at 100 °C and fired in an atmosphere of argon at 500 °C. The resulting monolith was black throughout the structure and when a sample was crushed none of the original pale cordierite structure was apparent. This suggests that the graphite/polymer slurry could have absorbed into the walls of the monolith. Vergunst et al. [38] have shown that a similar treatment results in carbon being present within the cordierite structure covering the walls of its macropores, as a thin layer on the external surface (wall) of the support, while the corners of the monolith channels are filled with more carbon. Gold was added as described for the carbon powder catalyst to achieve 1 wt%Au/C monolith catalyst.

2.2. Catalyst characterization

The 1 wt%Au/C powder catalyst has been characterized previously [28,29]. The major feature is that the impregnation treatment produced gold particles as small as 5 nm and as large as 50 nm in diameter, although the majority was 25 nm in size [29]. The preparation of the carbon cordierite monolith from the slurry of graphite and phenol formaldehyde resin produced a monolith where the carbon was present at a level of 8% on the total weight of the monolith. The Au/Carbon cordierite monolith was analyzed by electron probe micro-analysis (EPMA) and scanning and transmission electron microscopy (SEM, TEM). Secondary electron images from EPMA indicate a small layer adjacent to the monolith. The coating layer was observed to be made up of flakes (graphitic) of carbon. There was little evidence that the carbon had been absorbed into the cordierite, but the carbon did fill any recesses in the monolith as shown by SEM (Fig. 2). The thickness of the carbon layer varies over the monolith cells from what looks like nothing to thick areas in the corners (5–90 μm). Investigation of this layer by EPMA at low magnification revealed that it contained gold (Fig. 3) and high magnification suggests that the gold is in the form of particles. The catalyst was examined by TEM (Fig. 4) and Au particles as small as 20 nm and as large as 180 nm in diameter were observed, although the majority was 50 nm in size.

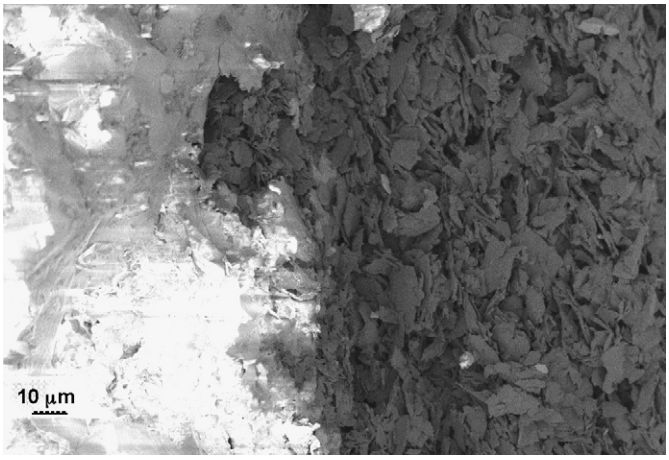

Fig. 2. Scanning electron microscopy data showing cordierite monolith (white) with carbon layer (brown).

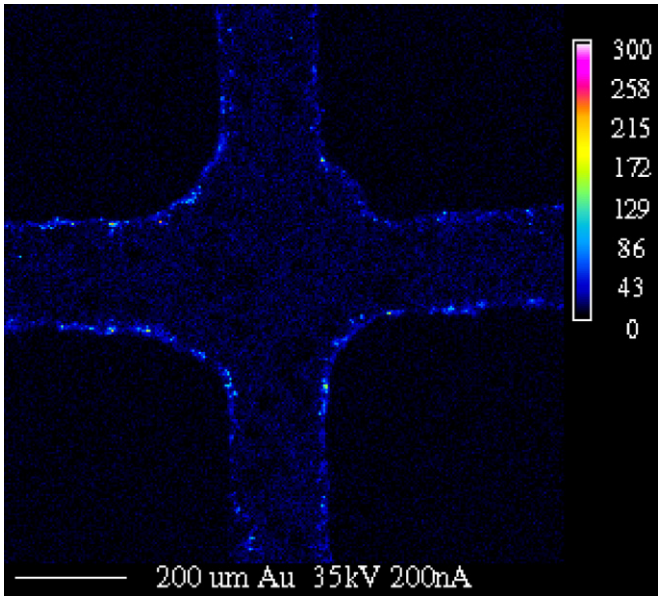

Fig. 3. Electron probe microanalysis probe micrograph at low magnification (120×) Peak-background corrected element (Au) distribution maps for 1 wt%Au/C on cordierite monolith.

2.3. Structured reactors

The structured reactors were tested in a laboratory scale loop reactor that has been described previously for hydrogenation reactions [7,39]. A brief description for oxidation is given here. All catalyst testing was carried out in a batch-recycle reactor, a schematic diagram of which is shown in Fig. 5. The reactor was

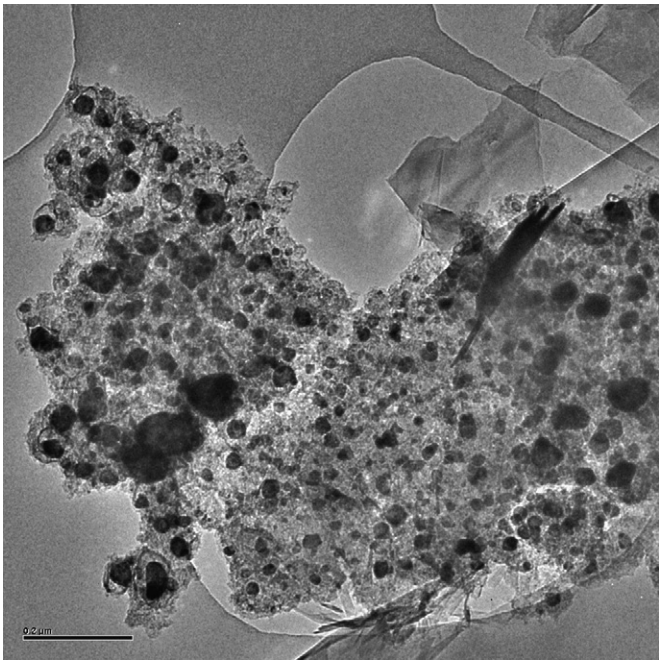

Fig. 4. Bright field transmission electron micrograph of 1 wt%Au/C on cordierite monolith.

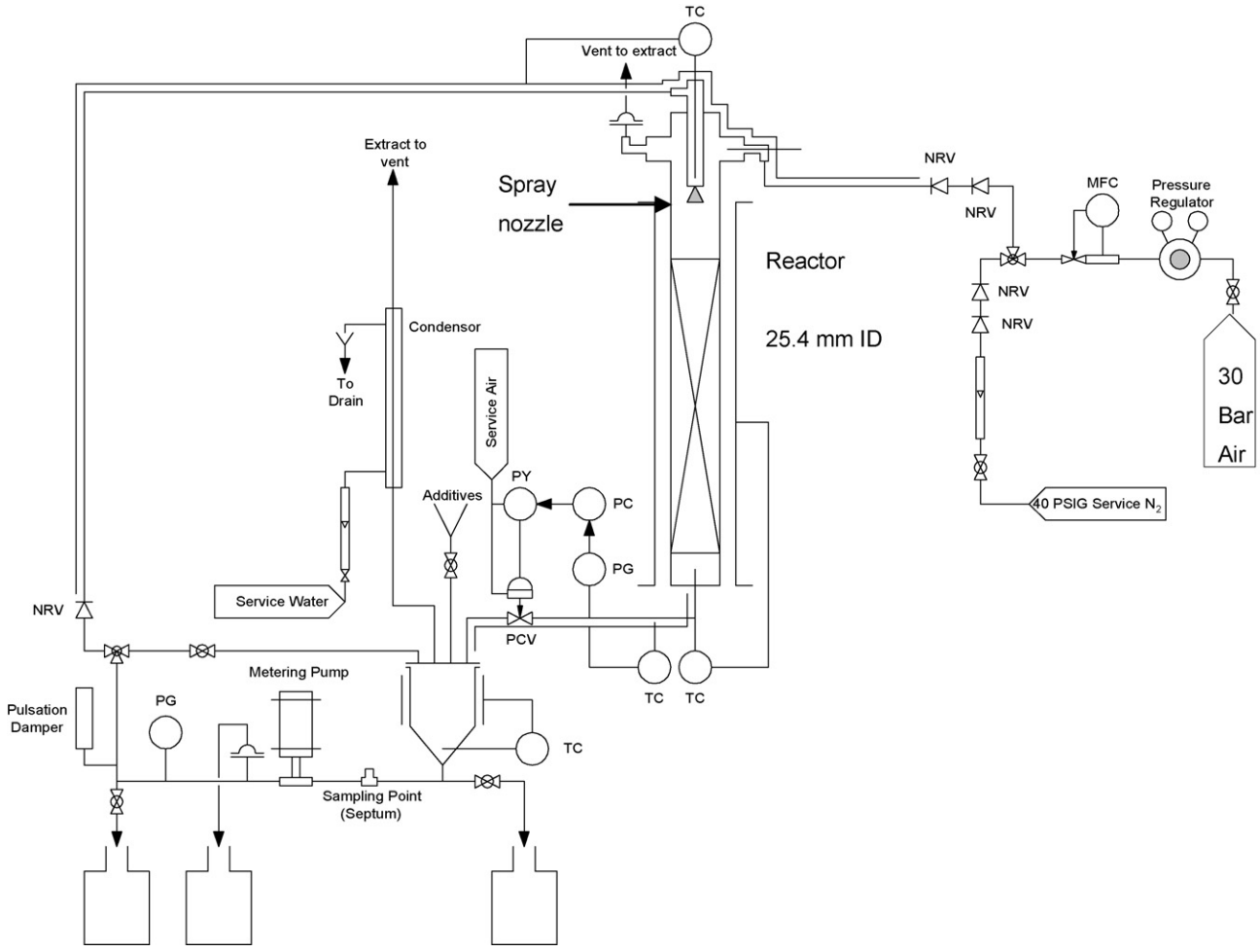

Fig. 5. Schematic diagram of batch recycle reactor.

designed for co-current downflow operation, liquid recirculation, and continuous gas feed. The liquid reactant (300 cm^3) was introduced into a receiver vessel (below additives on the diagram). The liquid reactant could be pumped from the receiver vessel around a closed loop by the use of a Bran + Luebbe H2-31 metering pump (0–80 L h^{-1}; discharge pressure 40 bar-g) or pumped to the reactor via a non-return valve. The liquid was introduced to the reactor using a spray nozzle to ensure a uniform flow distribution over the monolithic channels [40,41]. Air was introduced to the reactor from a compressed air gas cylinder using a Brooks 5850S mass flow controller (0–2 L min^{-1}) where it could be mixed with the liquid spray before the catalyst bed. The lines delivering liquid and gas reactants could be heated if appropriate. The reactor tube was 25.4 mm i.d. stainless steel tubing used to house the monolithic cores used for testing. The reactor was designed to operate at high temperature (250 °C) and high pressure (40 bar-g). A valve (PCV on Fig. 5) was incorporated to allow depressurization of the reactor exit flow. This enabled easy gas–liquid separation and sampling at atmospheric pressure. The liquid was recycled back to the receiver vessel and the air vented. The temperature was monitored by the use of thermocouples (TC on Fig. 5). The output from the thermocouples, gas mass flow controller, liquid metering pump controller, and pressure sensors was fed to a computer software package (SpecView, version 2). The software was designed in such a way that if there were any temperature or pressure excursions, the whole system could be shut down and the gas released safely. If such an incident occurred, nitrogen gas was used to purge the system before the operator could discharge the catalyst.

2.4. Catalyst testing

In all the tests the reactor vessel contained either an Au/C catalyzed monolith or a virgin cordierite monolith (62 channels per cm^2 (or 400 cpsi)). In the latter case the powder catalyst was placed in the receiver vessel with the liquid regent and thus, the catalyst flowed through the reactor dispersed as a powder in a gas–liquid flow, as a meso-structured downflow slurry bubble column. In the experiments with the Au/C catalyzed monolith, only the liquid reagent was placed in the receiver vessel. The conditions chosen for the tests were as close as possible to those in the earlier autoclave studies; glycerol (0.6 mol L^{-1}), glycerol/sodium hydroxide mol ratio 1:1, reaction temperature 60 °C, liquid–gas (air) ratio 1:1. The analysis of products was performed by HPLC [28,29].

3. Results

3.1. Catalyst activity

Studies of the oxidation of glycerol in the meso-structured SBCR and the catalyzed monolith reactor at 60 °C, at a pressure of 5 bar-a air, $p(O_2)$ 1 bar-a, at a superficial velocity of 5.6 mm s^{-1} are shown in Figs. 6 and 7. The conversion of glycerol was faster in the SBCR (30% after 24 min) compared with <20% conversion of glycerol in

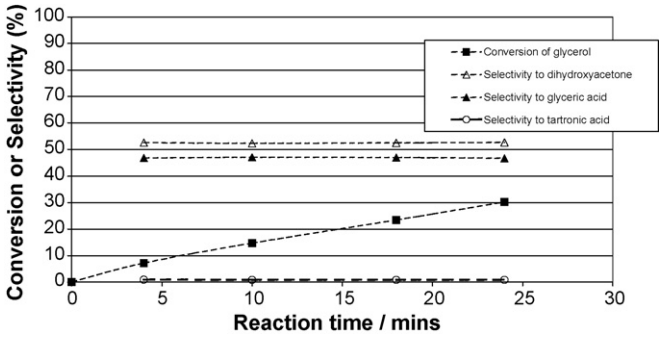

Fig. 6. Oxidation of glycerol over 1%Au/C catalyst in meso-structured SBCR. Experiment performed at a glycerol/metal mol ratio of 4730:1, temperature 60 °C, Air 5 bar-a, $p(O_2)$ 1 bar-a, liquid superficial velocity 5.6 mm s^{-1}, gas–liquid ratio of 1:1.

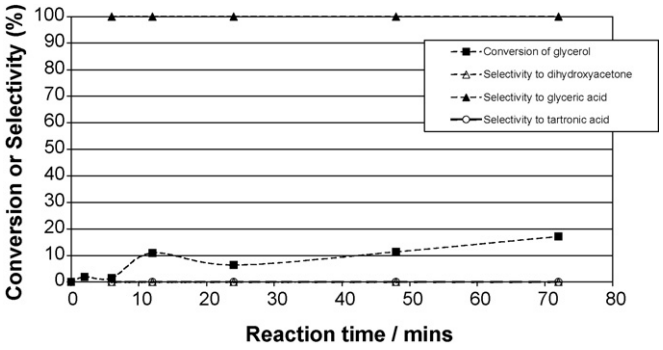

Fig. 7. Oxidation of glycerol over 1%Au/C catalyst on cordierite monolith. Experiment performed at a glycerol/metal mol ratio of 633:1, temperature 60 °C, Air 5 bar-a, $p(O_2)$ 1 bar-a, liquid superficial velocity 5.6 mm s^{-1}, gas–liquid ratio of 1:1.

70 min over the catalyzed monolith reactor. Total conversion of glycerol was observed after 70 min in the SBCR (not shown) at a higher partial pressure of oxygen, $p(O_2)$ 2.8 bar-a, in contrast to the slurry autoclave operation, which achieved less than 60% conversion after 180 min at a similar partial pressure of oxygen [28,29]. Previous studies have shown that full conversion of glycerol can be achieved over Au/C catalyst by optimizing the catalyst preparation method and the reaction conditions [30] and by the addition of Pt [33] or Pd [37]. The slurry catalyst in the structured SBCR was from the same batch as used for the autoclave experiments, and reaction conditions were also similar so the explanation for the difference in activity cannot be attributed to a different catalyst formulation.

Table 1 presents a summary of the experimental data from this study and from a sample autoclave experiment using the same slurry catalyst [29]. Rate data are presented in terms of both glycerol conversion and oxygen usage (calculated using the stoichiometry to obtain the observed products), based on both reactor volume and mass of gold. The structured SBCR shows the highest rates relative to both reactor volume and mass of gold. Most importantly, both the structured reactors, however, show higher rates than the stirred reactor. The reaction rates at the two lower oxygen partial pressures used in the structured SBCR are consistent with a first order dependency in oxygen partial pressure, whereas the autoclave studies show a partial order dependency. At the highest pressure, $p(O_2)$ 2.8 bar-a, the rate is significantly lower, and oxalic acid is observed, which infers over-oxidation of the catalyst.

Significantly lower rates are observed for the monolithic catalyst compared with the meso-structured slurry experiment. Indeed, when the monolith is crushed and tested in the autoclave reactor under the same conditions as used with the original Au/C powder catalyst [28,29] it is found to be less reactive. It must be noted that crushing the monolith may be detrimental for the Au/C coated catalyst. However, we consider that the material on the intact monolith is representative of this class of catalytic material and is therefore suitable for use in this comparative study. The data at lower oxygen partial pressures also indicate a partial order dependency similar to the autoclave studies, which suggests that the rate is not dominated but may be influenced by mass transfer (Fig. 8). The rate also increases with increasing phase velocity (Fig. 9) where the monolith and SSBCR show a similar and significant dependency. Hydrodynamic conditions for the monolith and structured SBCR are ostensibly the same and, could reasonably be expected to result in the same gas–liquid mass-transfer coefficient. The monolith runs would appear therefore to be more kinetically limited, inferring that the monolith catalyst is inherently less active than the slurry catalyst. The particle size of Au is larger on the carbon coated cordierite monolith compared to the slurry catalyst (~50 nm compared with ~25 nm). The influence of Au particle size for Au/C catalyst for glycerol oxidation has previously been investigated [30,32,36]. The conclusions from these studies were that activity increased with decreasing particle size but selectivity toward over-oxidation products also increased. However, the data presented in Table 1 also indicate that the volumetric rate of glycerol conversion is 10 times faster in the catalyzed monolith reactor compared with the autoclave studies. These results are considered very significant, since, we show, for the first time, that gold catalyzed reactions found to be relatively slow when conducted in a standard stirred batch reactor can be accelerated. Indeed, chemistry that seems slow in the lab (e.g. 24 h reaction times) is not necessarily actually slow when the reactor and reaction environment are properly engineered. Both monolith and meso-scale structured downflow slurry bubble column designs lead to a significant increase in the reaction rate

Table 1
Oxidation of glycerol using 1 wt%Au/C catalysts at 60 °C

Reactor	Gly/metal mol ratio	pO_2 (bar-a)	Superficial velocity (mm s^{-1})	Volumetric rate [Gly] (mmol s^{-1} m^{-3} bar^{-1})	Specific rate [Gly] (mmol s^{-1} g^{-1} bar^{-1})	Volumetric rate [O_2] (mmol s^{-1} m^{-3} bar^{-1})	Specific rate [O_2] (mmol s^{-1} g^{-1} bar^{-1})
Autoclave[a]	1080	3		4	0.09	4	0.09
Struct SBCR	4730	0.5	5.6	201	8.06	153	6.12
Struct SBCR	4730	1	5.6	195	7.81	143	5.74
Struct SBCR	4730	2.8	5.6	109	4.36	100	3.99
Monolith	633	1	5.6	36	0.10	36	0.10
Monolith	633	1	11	62	0.17	62	0.17
Monolith	633	1	17	65	0.18	65	0.18
Monolith	633	2.8	17	47	0.13	47	0.13
CM auto[b]	1080	3		0.6	0.01	1.4	0.03
CM auto[b]	4730	3		0.2	0.02	0.5	0.05

[a] Data taken from Carrettin et al. [29].
[b] CM auto (crushed monolith in autoclave, conditions as Carrettin et al. [29]).

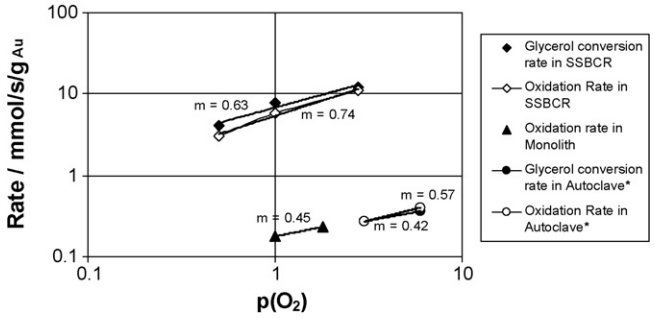

Fig. 8. Rate of oxidation of glycerol as a function of O_2 partial pressure in meso-structured SBCR, catalyzed monolith and slurry autoclave. Temperature 60 °C, gas–liquid ratio of 1:1. *Data taken from Carrettin et al. [29].

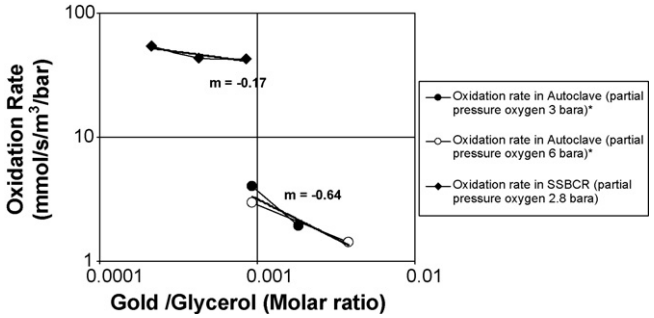

Fig. 10. Reaction rate as a function of gold:glycerol ratio. *Data taken from Carrettin et al. [29].

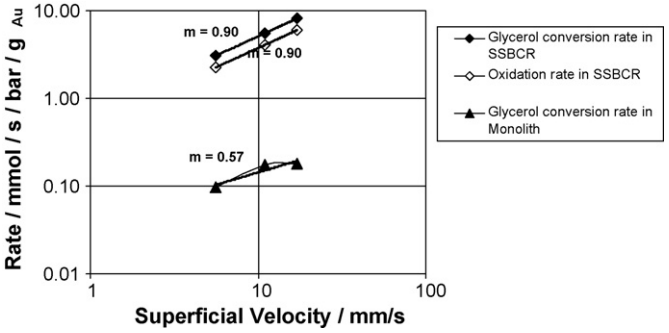

Fig. 9. Rate of oxidation of glycerol as a function of phase velocity in meso-structured SBCR and catalyzed monolith. Temperature 60 °C, gas–liquid ratio of 1:1.

over autoclave studies. In particular, the rate is an order of magnitude greater for the gold/carbon coated monolith, and increased by two orders of magnitude for the meso-scale structured downflow slurry bubble column reactor.

The reaction rate was investigated as a function of gold:glycerol ratio as shown in Fig. 10 for the meso-structured SBCR and slurry autoclave [29]. The reaction rate was found to be negative order with respect to catalyst and was consistent for two different reactors (autoclave and SBCR). This is most unusual and conflicts with results by Demirel-Gülen et al. [32] where the mass-transfer regime occurs below a glycerol/Au molar ratio of 2500. However, the results were obtained at different partial pressure of oxygen and base:glycerol ratio compared to their work. Our experimental studies compared glycerol to catalyst ratio keeping the base:-glycerol ratio constant at 1:1. Demirel-Gülen et al. [32] investigated increasing the glyercol:catalyst ratio whilst also keeping the base:glycerol concentration constant at 2:1. At low catalyst concentrations the initial reaction remains constant, which they attribute to the formation of foam. They also studied the effect of increasing base concentration whilst keeping the glycerol:catalyst ratio constant. An increase in the base concentration gave a greater conversion rate of glycerol, which is expected if base is responsible for deprotonation, which is the rate limiting step. Ketchie et al. [35] also studied the influence of base on oxidation of glycerol over Au. Their conclusions were that base was needed to deprotonate glycerol and that the immediate formed was oxidized by a predominantly surface catalyzed process. They also observed the formation of hydrogen peroxide at high pH. The formation of further oxidation products was attributed to the presence of hydrogen peroxide in solution. This indicates that an important relationship is apparent between base, glycerol and catalyst ratios and this will be studied further in subsequent investigations.

3.2. Selectivity of glycerol oxidation

The monolith and autoclave data show very high selectivity to glyceric acid; whereas, the thin channel bubble column yields approximately equal quantities of dihydroxyacetone and glyceric acid (Table 2). This cannot be attributed to different catalyst formulation, as the catalyst sample used in the autoclave work was the same batch as used for the thin channel bubble column reactor. Selectivity towards glyceric acid is reported to increase with increasing particle size [30,32]. The Au particle size on the monolith is larger than the powder catalyst. However, glyceric acid was the predominant product in the autoclave studies [28,29] whereas in the meso-structured reactor, dihydroxyacetone was also observed. The formation of secondary oxidation products as seen in the structured SBCR was also observed at the highest partial oxygen values in the autoclave [28,29]. This is indicative of higher oxygen availability in the structured SBCR compared to the autoclave and monolith reactors when all are operated at equivalent partial oxygen values. It is apparent therefore that

Table 2
Selectivity at 30% glycerol conversion

Reactor	Gly/metal mol ratio	pO_2 (bar-a)	Superficial velocity (mm s^{-1})	Glyceric acid	DHA	Tartronic acid	Oxalic acid
Autoclave[a]	1080	3		100	0	0	0
Struct SBCR	4730	0.5	5.6	52	47	1	0
Struct SBCR	4730	1	5.6	47	52	1	0
Struct SBCR	4730	2.8	5.6	42	53	0	5
Struct SBCR	2365	2.8	5.6	53	47	0	0
Struct SBCR	1165	2.8	5.6	54	46	0	0
Monolith	633	1	5.6	100	0	0	0
Monolith	633	1	11	100	0	0	0
Monolith	633	1	17	100	0	0	0
Monolith	633	2.8	17	100	0	0	0

[a] Data taken from Carrettin et al. [29].

the structured SBCR facilitates the faster oxygen transport. Kimura et al. [25] studied the selective oxidation of glycerol with air on a platinum catalyst at atmospheric pressure and found that an improved selectivity towards dihydroxyacetone with the addition of bismuth promoter. It is also interesting to note that Demirel et al. [33] could improve selectivity to dihydroxyacetone over a Au/C catalyst with the addition of platinum, which also increased the activity. In our system this effect occurred by placing the Au/C in a meso-scale structured environment. The difference in selectivity can be attributed to the interaction between bubbles and particles, and meso-scale structuration as described earlier. It is also interesting to note that the inherently less active monolith catalyst gives 100% selectivity to glyceric acid and at a higher volumetric rate of reaction under milder conditions compared to autoclave studies.

4. Conclusions

We have shown that oxidation using gold catalysts can be performed at high rates under mild conditions in continuous flow structured reactors. The performance of the slurry catalyst in the meso-structured downflow slurry bubble column reactor showed that performance benefits can be obtained by structuring gas–liquid–solid reacting flows in thin channels or capillaries. The meso-structured downflow slurry bubble column reactor gave a different product distribution compared to the stirred tank and monolith inferring higher oxygen availability. This is attributed to enhanced interaction between bubbles and particles from meso-scale structuration.

Acknowledgements

This work was carried out as part of the ATHENA project funded by the EPSRC. Dr. Landon would like to thank the Engineering and Physical Sciences Research Council UK (EPSRC) for the funding of the Research Associate Industrial Secondments, which was carried out at Johnson Matthey, Billingham UK. Prof. Stitt, Dr. Wagland and Dr. Pollington would thank to thank Johnson Matthey for permission to publish the work. The authors also thank the Analytical Department at Johnson Matthey Technology Centre, Sonning Common for the characterization studies on the monolith.

References

[1] F. Kapteijn, J.J. Heiszwolf, T.A. Nijhuis, J.A. Moulijn, CATTECH 3 (1999) 24–41.
[2] M.T. Kreutzer, F. Kapteijn, J.A. Moulijn, Catal. Today 111 (2006) 111–118.
[3] R.M. Machado, R.R. Broekhuis, A.F. Nordquist, B.P. Roy, S.R. Carney, Catal. Today 105 (2005) 305–317.
[4] S. Roy, T. Bauer, M. Al-Dahhan, P. Lehner, T. Turek, AIChE J. 50 (2004) 2918–2938.
[5] Chemical Week, September 3, 2003.
[6] A.M. Chem, Eng. News 81 (July 14, 2003) 48. FlexPlant—Flexible Laboratory Process Intensification Plant. http://www.bhrgroup.co.uk/pi/flexplant.htm.
[7] D.I. Enache, G.J. Hutchings, S.H. Taylor, R. Natividad, S. Raymahasay, J.M. Winterbottom, E.H. Stitt, Ind. Eng. Chem. Res. 44 (2005) 6295–6303.
[8] D.I. Enache, G.J. Hutchings, S.H. Taylor, E.H. Stitt, Catal. Today 105 (2005) 569–573.
[9] J.J. Lerou, K.M. Ng, Chem. Eng. Sci. (1996) 1595–1614.
[10] D.I. Enache, G.J. Hutchings, S.H. Taylor, S. Raymahasay, J.M. Winterbottom, M.D. Mantle, A.J. Sederman, L.F. Gladden, C. Chatwin, K.T. Symonds, E.H. Stitt, Catal. Today 128 (2007) 26–35.
[11] M.T. Kreutzer, J.J.W. Bakker, F. Kapteijn, J.A. Moulijn, Ind. Eng. Chem. Res. 44 (2005) 4898–4913.
[12] R. Krishna, Oil Gas Sci. Tech. Rev. 55 (2000) 359–393.
[13] B. Hu, A.W. Pacek, E.H. Stitt, A.W. Nienow, Chem. Eng. Sci. 60 (2005) 6371–6377.
[14] K.C. Ruthiya, J. van der Schaaf, B.F.M. Kuster, J.C. Schouten, Chem. Eng. Sci. 59 (2004) 5551–5558.
[15] L.F. Gladden, M.H. Lim, M.D. Mantle, A.J. Sederman, E.H. Stitt, Catal. Today 79/80 (2003) 203–210.
[16] A.J. Sederman, J.J. Heras, M.D. Mantle, L.F. Gladden, Catal. Today 128 (2007) 3–12.
[17] A.N. Tsoligkas, M.J.H. Simmons, J. Wood, C.G. Frost, Catal. Today 128 (2007) 36–46.
[18] P.L. Mills, R.V. Chaudhari, Catal. Today 37 (1997) 367–404.
[19] R.A. Sheldon, R.S. Downing, Appl. Catal. A: Gen. 189 (1999) 163–183.
[20] R.A. Sheldon, I.W.C.E. Arends, A. Dijksman, Catal. Today 57 (2000) 157–166.
[21] G.-J. Ten Brink, I.W.C.E. Arends, R.A. Sheldon, Science 287 (5458) (2000) 1636–1639.
[22] W.F. Hoelderich, Catal. Today 62 (2000) 115–130.
[23] A.S.K. Hashmi, G.J. Hutchings, Angew. Chem. Int. Ed. 45 (2006) 7896–7936.
[24] T. Mallat, A. Baiker, Catal. Today 24 (1995) 143–150.
[25] H. Kimura, K. Tsuto, T. Wakisaka, Y. Kazumi, Y. Inaya, Appl. Catal. A: Gen. 96 (1993) 217–228.
[26] H. Kimura, Appl. Catal. A: Gen. 105 (1993) 147–158.
[27] P. Fordham, R. Garcia, M. Besson, P. Gallezot, Stud. Surf. Sci. Catal. 101 (1996) 161–170.
[28] S. Carrettin, P. McMorn, P. Johnston, K. Griffith, G.J. Hutchings, Chem. Commun. (2002) 696–697.
[29] S. Carrettin, P. McMorn, P. Johnston, K. Griffith, C.J. Kiely, G.J. Hutchings, Phys. Chem. Chem. Phys. 5 (2003) 1329–1336.
[30] F. Porta, L. Prati, J. Catal. 224 (2004) 397–403.
[31] C.L. Bianchi, P. Canton, M. Dimitratos, F. Porta, L. Prati, Catal. Today 102/103 (2005) 203–212.
[32] S. Demirel-Gülen, M. Lucas, P. Claus, Catal. Today 102/103 (2005) 166–172.
[33] S. Demirel, K. Lehnert, M. Lucas, P. Claus, Appl. Catal. B: Environ. 70 (2007) 637–643.
[34] G.J. Hutchings, S. Carrettin, P. Landon, J.F. Edwards, D.I. Enache, D.W. Knight, X.-J. Xu, A.F. Carley, Top. Catal. 38 (2006) 223–230.
[35] W.C. Ketchie, M. Murayama, R.J. Davis, Top. Catal. 44 (2007) 207–317.
[36] W.C. Ketchie, Yu-L. Fang, M.S. Wong, M. Murayama, R.J. Davis, J. Catal. 250 (2007) 94–101.
[37] W.C. Ketchie, M. Murayama, R.J. Davis, J. Catal. 250 (2007) 264–273.
[38] Th. Vergunst, F. Kapteijn, J.A. Moulijn, Carbon 40 (2002) 1891–1902.
[39] D.I. Enache, P. Landon, C.M. Lok, S.D. Pollington, E.H. Stitt, Ind. Eng. Chem. Res. 44 (2005) 9431–9439.
[40] S. Irandourst, A. Andersson, Ind. Eng. Chem. Res. 28 (1989) 1684–1688.
[41] T.A. Nijhuis, M.T. Kreutzer, A.C.J. Romijn, F. Kapteijn, J.A. Moulijn, Chem. Eng. Sci. 56 (2001) 823–829.